

NJC

Accepted Manuscript



This article can be cited before page numbers have been issued, to do this please use: F. Aribi, A. Panossian, D. Jacquemin, J. Vors, S. Pazenok, F. R. Leroux and M. Elhabiri, *New J. Chem.*, 2018, DOI: 10.1039/C8NJ00916C.



This is an Accepted Manuscript, which has been through the Royal Society of Chemistry peer review process and has been accepted for publication.

Accepted Manuscripts are published online shortly after acceptance, before technical editing, formatting and proof reading. Using this free service, authors can make their results available to the community, in citable form, before we publish the edited article. We will replace this Accepted Manuscript with the edited and formatted Advance Article as soon as it is available.

You can find more information about Accepted Manuscripts in the [author guidelines](#).

Please note that technical editing may introduce minor changes to the text and/or graphics, which may alter content. The journal's standard [Terms & Conditions](#) and the ethical guidelines, outlined in our [author and reviewer resource centre](#), still apply. In no event shall the Royal Society of Chemistry be held responsible for any errors or omissions in this Accepted Manuscript or any consequences arising from the use of any information it contains.



Journal Name

ARTICLE

A Physico-chemical Investigation on Fluorine-Enriched Quinolines

Fallia Aribi,^{a,b} Armen Panossian,^{a,b} Denis Jacquemin,^c Jean-Pierre Vors,^{b,d} Sergii Pazenok,^{b,e} Frédéric R. Leroux^{*a,b} and Mourad Elhabiri^{*a}

Received 00th January 20xx,
Accepted 00th January 20xx

DOI: 10.1039/x0xx00000x

www.rsc.org/

Quinoline derivatives bearing fluoroalkyl groups at both 2 and 4 positions are scarcely described in the literature. Nevertheless, the addition of fluorine onto the quinoline core might bring new interesting physico-chemical properties. To confirm this hypothesis a homogenous series of 2,4-bis(fluoroalkyl)-substituted quinolines was synthesized under mild reaction conditions and their physico-chemical properties were thoroughly investigated by various techniques to illustrate their potential usefulness as new building blocks for applications ranging from organic chemistry to material science.

Introduction

Since their discovery in 1834 by F. Runge, quinoline cores have enjoyed a huge success in several fields, notably, medicinal chemistry^[1] like antimalarial (Primaquine[®]) or anti-tumoral (Lenvima[®]) drugs, local anaesthetics (Nupercainal[®]), agrochemistry^[2] as fungicides (Fortress[®]) and herbicides (Pestanal[®]) as well as in materials science^[3] (Figure 1). For more than 150 years, the synthesis of quinoline derivatives has been explored and many methods are now available to access them. The oldest reaction is the so-called Skraup synthesis developed in 1880,^[4] but, several alternative methods have been developed, *e.g.*, the Doebner-Von Miller reaction,^[5] the Conrad-Limpach synthesis,^[6] the Friedländer reaction,^[7] the Pfitzinger reaction,^[8] the Combes reaction,^[9] and the Meth-Cohn synthesis.^[10] Most of these methods involve simple to complex aryl-amines or related substrates as starting materials.^[11]

Other metal-free reactions, combining high yields and short reaction times, were also proposed.^[12] Later, metals like rhodium, platinum, copper, palladium, iron and others allowed the formation of quinoline derivatives using catalytic amounts of metal.^[13] While quinolines are valuable scaffolds, fluorine is an important heteroatom in life science, since it can improve the physico-chemical properties of a bioactive molecule, *e.g.*, by altering the acido-basic properties of proximate groups, by increasing the lipophilicity of the molecule, or by improving its stability toward oxidative degradation.^[14] Therefore, the

introduction of fluorinated moieties onto quinoline derivatives has become an increasingly attractive target in several chemical areas.

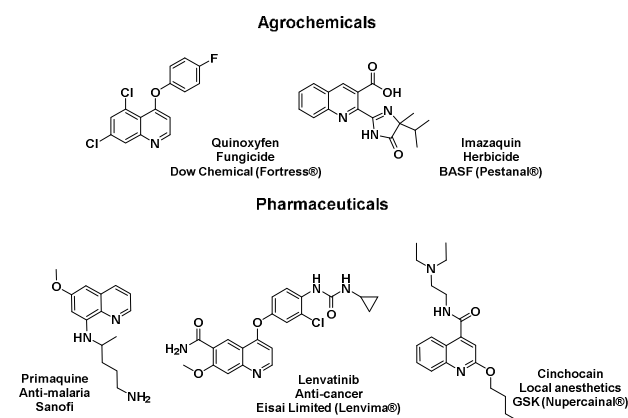


Figure 1. Commercially available quinolines as agrochemicals and pharmaceuticals.

However, reaching this goal constitutes a significant challenge. The introduction of fluorine onto heteroarenes is usually performed thanks to the Balz-Schiemann reaction, the Halex process, or by using fluorinating agents,^[15] whereas perfluoroalkyl groups can be introduced by classical nucleophilic fluorination following a Swarts-type reaction in presence of HF or SbF₅ or using nucleophilic (Ruppert-Prakash reagent) or electrophilic (Umemoto or Togni reagents) techniques.^[16] However, most of these methods allow the insertion of only one fluorinated substituent onto quinolines. In the literature, only a limited number of works reported the synthesis of quinoline derivatives bearing several fluorinated substituents. In 2002, Sloop *et al.*^[17] and then in 2012, Baran *et al.*^[18] performed the synthesis of quinolines bearing fluoroalkyl substituents at both C2 and C4 positions. Nevertheless, such compounds are generally obtained in low yields or with a poor

^a Université de Strasbourg, Université de Haute-Alsace, CNRS (ECPM), UMR 7042-LIMA, 25 Rue Becquerel, 67000 Strasbourg, France. E-mail: frederic.leroux@unistra.fr and elhabiri@unistra.fr

^b Joint laboratory Unistra-CNRS-Bayer (Chemistry of Organofluorine Compounds), France.

^c Laboratoire CEISAM - UMR CNRS 6230, CNRS – Université de Nantes, 2 rue de la Houssinière, 44322 Nantes, Cedex 3, France

^d Bayer S.A.S, 14 Impasse Pierre Baizet, BP99163, 69263 Lyon Cedex 09, France.

^e Bayer AG, Alfred-Nobel-Strass 50, 40789 Monheim, Germany

Electronic Supplementary Information (ESI) available: [Absorption data; emission data; cyclic voltammetry data; DFT calculations]. See DOI: 10.1039/x0xx00000x

ARTICLE

Journal Name

regioselectivity due to the use of unsymmetrical reactants. Recently, we developed a new, efficient, mild and completely regioselective method allowing to access, from readily available starting materials, to scarcely described polyfunctionalized fluoroalkylated quinolines.^[19] The strategy is based on the use of FARs (Fluoroalkyl Amino Reagents) (Figure 2).^[20]

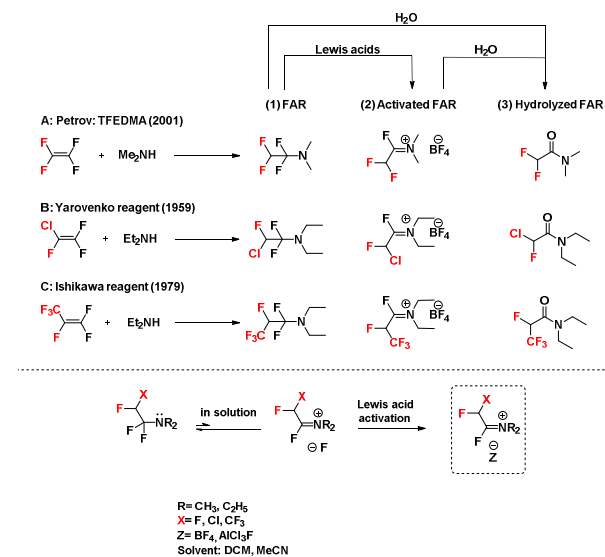


Figure 2. Commercially available Fluoroalkyl Amino Reagents (FARs) [Top]; Activation of FARs by Lewis acids converting them into their corresponding iminium salts [Bottom].

This synthesis consists in a two-step reaction; the first corresponds to the condensation of anilines onto fluorinated ketones to provide fluorinated *N*-aryl acetimines. The latter intermediate is an analogue of the one formed during the Meth-Cohn synthesis, which uses the Vilsmeier reagent.^[21] In the second step, the vinamidinium intermediate further cyclises into quinolines after electrophilic aromatic substitution and rearomatization following a Combes-like cyclization process (Figure 3, Scheme 1).

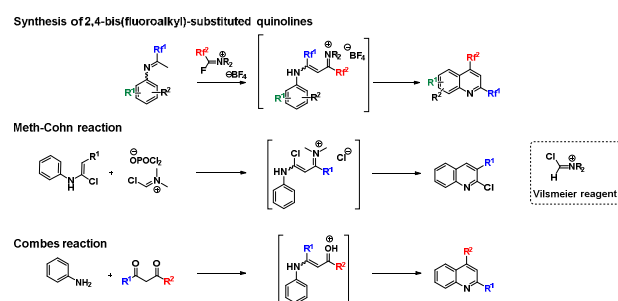
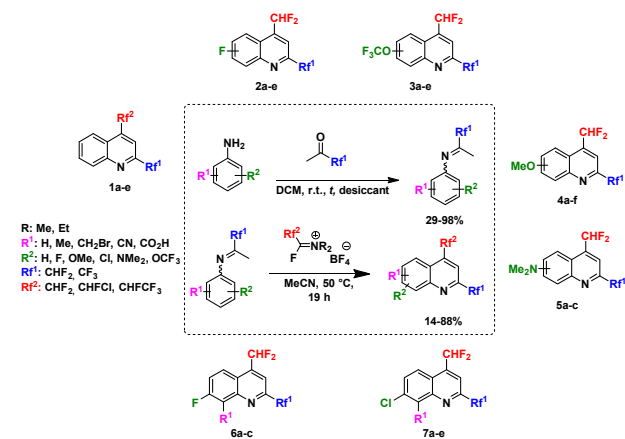


Figure 3. Analogy with the Meth-Cohn and the Combes syntheses.



Scheme 1. Synthetic routes to fluorinated quinolines and chemical structures and labelling of the investigated compounds.

In a previous contribution,^[19] we reported on the reactivity of these quinoline derivatives towards further functionalization. In fact, they can be hardly oxidized and require harsh reaction conditions presumably due to their low electron-density. To confirm this hypothesis, we performed electrochemical studies on a homogenous series of quinoline derivatives to determine their physico-chemical properties, and we concomitantly carried out spectrophotometric (absorption and emission) analyses. Indeed, some of these compounds, and more specifically those substituted by electron-donating groups, were found to be brightly fluorescent in solution. Density Functional Theory (DFT) and Time-Dependent DFT (TD-DFT) calculations allowed assessing and rationalizing the experimental data. To the best of our knowledge, similar complementary analyses were not performed on this type of compounds so far.

Results and Discussion

Spectroscopic properties. In small aromatic molecules containing one or two six-membered cycles, three sets of absorption bands, corresponding to π - π^* transitions, are usually observed in the near UV region. According to Platt's theory and notation,^[22] these absorptions can be ascribed to transitions from the 1A_g ground state to 1L_a , 1L_b and 1B_b electronic excited states. These π - π^* absorption bands are generally labelled III ($^1A_g \rightarrow ^1B_b$ lowest excited state of B_{3u} symmetry), II ($^1A_g \rightarrow ^1L_a$, lowest excited state of B_{2u} symmetry) and I ($^1A \rightarrow ^1L_b$, lowest excited-state of B_{3u} symmetry), the latter is forbidden by symmetry and associated with weak absorptivities.^[23] The 1L_a excited state typically corresponds to a HOMO \rightarrow LUMO electronic promotion with large polarization and energy along the short molecular y axis, while the 1L_b excited state is characterized by a nearly equal admixture of HOMO-1 \rightarrow LUMO and HOMO \rightarrow LUMO+1 characters with a total polarization along the long x axis (Figure 4, Figure 5 and Figure S1, ESI).^[23b, 24] It is noteworthy that the configuration interaction between HOMO-1 \rightarrow LUMO and HOMO \rightarrow LUMO+1 is large enough to bring the energy of the 1L_b below

HOMO→LUMO (1L_a) transition. Therefore, in naphthalene, the lowest singlet excited state corresponds to a HOMO-1→LUMO and HOMO→LUMO+1 combination rather than a HOMO→LUMO transition (Figure 4 and Figure 5).

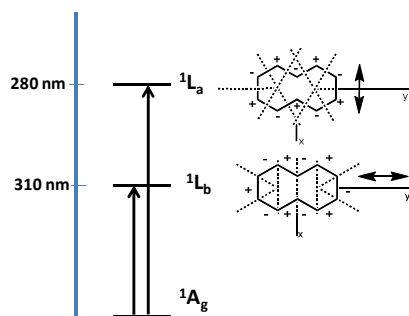


Figure 4. Electronic energy diagrams of naphthalene molecular orbitals and polarization diagrams for the two lowest absorption bands I and II.

Quinolines are heteroaromatic nitrogen heterocycles that are structurally equivalent and π -isoelectronic to naphthalene. While the absorption spectrum of isoquinoline is similar to that of naphthalene, that of quinoline is markedly different. This can be ascribed to the inductive perturbation of the electronegative α -nitrogen atom (Figure S1, ESI) as well as the significant change in the relative positions of MO energy levels.^[23a] Quinoline exhibits two strong absorption bands (III and IV) instead of the 1B_b band of naphthalene, whose maxima are centered at *ca.* 226 nm (in $C_2H_4Cl_2$, Figure 5) and 203 nm, respectively.^[23a] In addition, the first (1L_b) and second (1L_a) absorption bands, that are more easily accessible in the UV-visible window of the spectrum, are poorly separated from each other. Transition from the ground state to the 1L_a state usually gives rise to a broad absorption, while transition to the 1L_b state results in a sharp and fine structured absorption showing a hallmark vibronic progression, Figure S2, ESI).

Lastly, the absorptivity of the quinoline 1L_b absorption is significantly increased with respect to that of naphthalene as the transition moment of 1L_b band is almost parallel to the long axis of the molecule and also due to a contribution of the 1B_b state.^[25] Finally, the $n \rightarrow \pi^*$ transitions that can be anticipated for heteroaromatic nitrogen heterocycles like quinoline are “forbidden” by symmetry ($\epsilon \leq 100 \text{ M}^{-1} \text{ cm}^{-1}$) and are therefore usually buried under the intense $\pi \rightarrow \pi^*$ transitions.

Substitution of positions C2 and C4 of the quinoline (pyridyl unit) by fluorinated alkyl groups (*e.g.* CHF_2 , $CHCl$, CF_3 or $CHFCl_2$) alters the electronic absorption spectrum (Figure S1, ESI). Indeed, both the 1L_b (band I) and 1L_a (band II) $\pi \rightarrow \pi^*$ transitions experience bathochromic displacements of *ca.* 7 and 15 nm (Figure 5) with respective hypo- and hyperchromic shifts (Figures S1 and S3, ESI). These effects contribute to blend even more these two sets of transitions that appeared closer from one another (Figure 5).

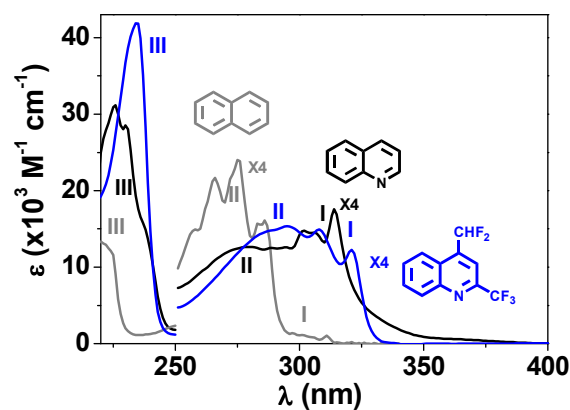


Figure 5. Comparison between the electronic absorption spectra of naphthalene (cyclohexane)^[26], quinoline (1,2-dichloroethane) and **1a** (1,2-dichloroethane) measured at 25 °C.

A significant increase of the absorptivity of band III, that is red shifted, is observed as well. Additionally, no significant influence of the nature of substitution was observed (CHF_2 versus $CHCl$ versus CF_3 versus $CHFCl_2$, Figure S3 and Table S1, ESI). The fact that the shape of the electronic absorption spectra did not vary with respect to the fluorine substitution pattern on either position 2 or 4 suggests that adding a limited number of this strong -I atom ($\sigma_m = +0.34$),^[27] is sufficient to obtain the largest possible effect.

We next examined the effect of fluorine-group substitution on the benzene-type unit of derivatives **1a** and **1d**. More in details, fluorine and trifluoromethoxy groups were introduced either at the C6 (**2a**, **2d** for F and **3a**, **3c** for OCF_3), C7 (**2b**, **2e** for F and **3b**, **3d** for OCF_3) or C8 (**2c** for F and **3e** for OCF_3) positions, while the pyridyl substitution pattern was conserved with either CHF_2/CF_3 (**1a** series) or CHF_2/CHF_2 (**1d** series). Regardless of the considered system (**1a** or **1d**), the introduction of a fluorine or trifluoromethoxy unit on either C6 or C7 positions led to a significant hypochromic shift of band III with a gradual hypsochromic shift (Tables S2-S5 and Figures S4-S7, ESI) compared to the unsubstituted (**1a** or **1d**) structures. In contrast, substitution at the C6 position has only a weak impact on the position and shapes of bands I (1L_b) and II (1L_a), but a more noticeable effect on their absorptivities. In other words, fluorine-based groups substituted at the C6 position weakly influences the two low 1L_a and 1L_b electronic transitions of the **1a** and **1d** quinoline chromophore. Interestingly, substitution at the C7 position has a larger effect on both the 1L_a (hypsochromic shift) and 1L_b (bathochromic shift) transitions contributing to split these two sets of absorptions. These effects can be ascribed to the π -electron donor (+M) character of F which stabilizes the 1L_b state (*i.e.*, bond-centered excess charge density character) but destabilizes the 1L_a state (*i.e.*, atom-centered excess charge density). Substitution of a fluorine atom at C8 stands in an interesting contrast with a blending of the 1L_b and 1L_a transitions suggesting that inductive effects (-I) of the substituent govern the response in that case.

ARTICLE

Journal Name

For the OCF_3 group ($\sigma_m = +0.38$ and $\sigma_p = +0.35$, strong electron withdrawer $-I$ and weak π -electron donor $+M$), a hypsochromic effect of the 1L_a band can be observed after substitution at the C6 or C7 positions of either **1a** or **1d** quinolines series, while the 1L_b absorption remains unaffected. Strikingly, substitution at the C8 position has a weak or trifling effect.

To study the impact of the nature of the substitution at C6, we selected compound **1a** (Scheme 1) as the reference scaffold. The electronic absorption spectra of the F (**2a**), OCF_3 (**3a**), OCH_3 (**4a**) and NMe_2 (**5a**) derivatives of **1a** are depicted in Figure 6.

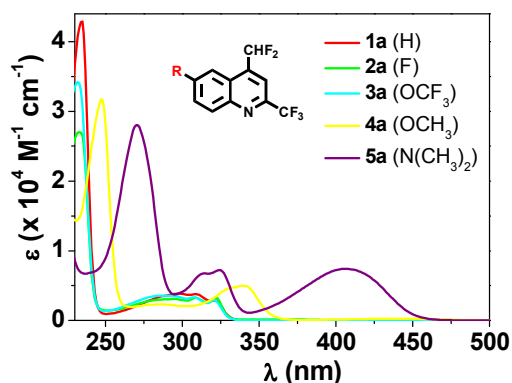


Figure 6. Influence on the absorption spectra of the substitution on the C6 position for quinoline derivatives bearing a CF_3 in C2 and a CHF_2 in C4 (derivative **1a** as a scaffold reference). Solvent: 1,2-dichloroethane, $T = 25.0(2)^\circ\text{C}$.

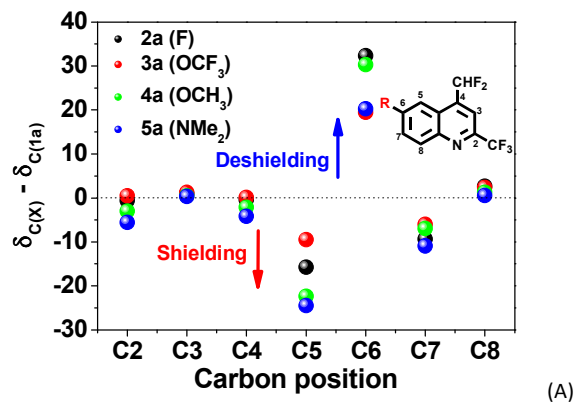
As discussed above, substitution by fluorinated groups such as F (**2a**) or OCF_3 (**3a**) induces minor changes of the absorption bands of the quinoline (Figure 6 and Table S6, ESI). By contrast, the OCH_3 (**4a**) and NMe_2 (**5a**) substituents, that display strong mesomeric effects ($\sigma_p = -0.27$ and $\sigma_m = 0.12$ for OCH_3 and $\sigma_p \sim -0.83$ and $\sigma_m = -0.15$ for NMe_2), lead to marked alterations of the absorption properties of the quinoline. Band III experienced strong bathochromic and hypochromic shifts, concomitantly to significant alterations of both the shape and position of bands I (1L_b) and II (1L_a). In particular, for the dimethylamino derivative, a broad and intense absorption emerges in the UV-visible region, which is typical of a change from a local excited state to an intramolecular charge-transfer (ICT) excited state (see TD-DFT calculations, *vide infra*).

For 6-substituted quinolines with strong π electron-donating substituents, ${}^{13}\text{C}$ NMR studies^[28] revealed marked upfield shifts of the *ortho*-carbons and minor upfield shifts of the *para*-carbon (*i.e.*, with respect to the C6 position) for the phenyl ring, whereas the changes were negligible for the pyridyl moiety. On the other hand, the absorption spectrum of 6-dimethylamino-quinoline recorded in methanol,^[29] depicted absorptions at *ca.* 250, 295, and 380 nm, whereas the acidification of a methanolic solution (0.01 N HCl), leading to the protonation of the *N*-quinoline unit, shifted the main absorption bands to 270, 300 and 440 nm, respectively.

Furthermore, a spectroscopic study of 5-substituted quinolines in aqueous solutions showed that their photobasicity can be magnified and controlled by tuning the relative energies of the 1L_a states of the acid and base forms.^[30] The 1L_a transitions shifted from *ca.* 370 nm to *ca.* 457 nm when going from the neutral to the protonated 5-aminoquinoline leading to the highest ΔpK_a separation ($pK_a^* - pK_a = 10.6$).

Based on these reported investigations, we anticipated that the absorption lying at 406 nm ($\epsilon^{406} = 7.4 \times 10^3 \text{ M}^{-1} \text{ cm}^{-1}$) for **5a** (*i.e.*, under deprotonated form in pure 1,2-dichloroethane) corresponds to the 1L_a transition (with an ICT character), while those centered at 324 nm ($\epsilon^{324} = 7.24 \times 10^3 \text{ M}^{-1} \text{ cm}^{-1}$) and 270 nm ($\epsilon^{270} = 2.8 \times 10^4 \text{ M}^{-1} \text{ cm}^{-1}$) correspond to bands I (1L_b) and III, respectively.

Regardless of the considered solvent (methanol^[29] or 1,2-dichloroethane), the presence of the fluorinated substituents at C2 and C4 positions induces a further bathochromic shift of *ca.* 20 nm of the main absorption bands for **5a** compared to the reference 6-dimethyl-amino-quinoline (*vide supra*).^[29] Furthermore, despite the absence of mesomerism between N1 and NMe_2 in **5a**, a large (moderate) red shift of the 1L_a (1L_b) absorption is observed, suggesting a ground state electronic perturbation likely confined to the benzene ring as suggested by previous ${}^{13}\text{C}$ NMR for 6-substituted quinolines.^[28] To get further insights into these electronic effects, ${}^{13}\text{C}$ NMR chemical shifts of **1a** and its C6-substituted analogues (**2a**, **3a**, **4a** and **5a**) were recorded in CDCl_3 (Table S7 and Figures S30-S34, ESI). Figure 7 illustrates the variations of the chemical shifts of the quinoline carbons as a function of the nature of substitution at the C6 position for the **1a** and the quinoline^[28] series, respectively. As a consequence of the sizeable $-I$ effect of the F and OCF_3 substituents, the ${}^{13}\text{C}$ δ of the C6 carbon is deshielded (lower electron density), while the neighbouring carbons (C5 and C7) are concomitantly shielded. The ${}^{13}\text{C}$ chemical shifts of the other carbons belonging either to the pyridine subunit or far from the C6 position, *e.g.*, C8, are unaffected. We note that fluorinated substitution induces marked effects compared to substitution with other halogens such as Br ($\sigma_p = 0.23$ and $\sigma_m = 0.39$) or Cl ($\sigma_p = 0.23$ and $\sigma_m = 0.37$) (Figure 7B).^[28] This feature agrees with our absorption data and suggests the absence of ICT in the whole aromatic system for these substitutions.



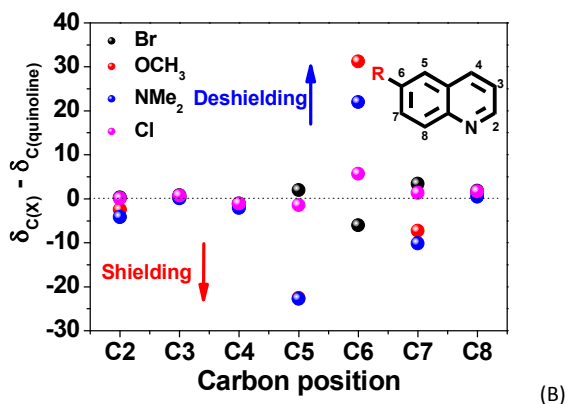


Figure 7. Variation of the ^{13}C NMR shifts of the quinoline carbon atoms as a function of the nature of the substituent on position C6. (A) **1a** series, this work; (B) quinoline; ref. ^[28]. Solvent: CDCl_3 ; $T = 298\text{ K}$.

For the OCH_3 (**4a**) and NMe_2 (**5a**) derivatives, the same trends are found with, however, apparent shielding effects of the ^{13}C signals of the C2 and C4 carbons, suggesting resonance process along the whole aromatic system and therefore an ICT character. This is in line with the large bathochromic shifts evidenced for the $^1\text{L}_a$ transitions of **4a** and **5a** as well as with TD-DFT calculations (*vide infra*). For the C2- and C4-unsubstituted quinolines (Figure 7B),^[28] substitution by a NMe_2 group at the C6 position also induce a shielding of the C2 position likely as a result of this resonance effect. The C2 and C4 substitutions with electron withdrawing fluorinated functions exacerbate this electronic effect with respect to quinoline (Figure 7A/B).

The **1d** series (CHF_2 at C2 and C4 positions) was also considered and the absorption electronic spectra of the 6-substituted derivatives with F (**2d**), OCF_3 (**3c**), OCH_3 (**4d**) and NMe_2 (**5b**) groups can be found in Table S10 and Figure S10. Overall, the auxochromic effects discussed for the **1a** series hold in the **1d** series. The substitution pattern (CF_3 versus CHF_2) on the pyridyl ring (**1d** versus **1a**) does not modify the spectral variations induced by the substituents at the C6 position. The F (**2d**) and OCF_3 (**3c**) substitutions at the C6 position of the **1d** backbone induce only minor alterations on the absorptions I, II and III (*vide infra*). Furthermore, the $^1\text{L}_a$ transitions are bathochromically shifted to 446 nm ($\epsilon^{446} = 934\text{ M}^{-1}\text{ cm}^{-1}$) and 400 nm ($\epsilon^{400} = 6.93 \times 10^3\text{ M}^{-1}\text{ cm}^{-1}$) for **4d** (6-methoxy) and **5b** (6-dimethylamino), respectively. For all series, the C6- OCH_3 substitution yields weaker absorptivity for the absorption lying at low energies compared to the NMe_2 substitution. This suggests a process controlled by both inductive (-I, $\sigma_m = +0.12$) and mesomeric (+M, $\sigma_p = -0.27$) effects for OCH_3 , while for NMe_2 $\sigma_m = -0.15$, $\sigma_p = -0.83$), the mesomer donating effect dominates. For the OCH_3 substitution, this is further shown by the large red shift of the $^1\text{L}_b$ transitions.

The ^{13}C NMR investigation (Table S8, Figure S8 and Figures S35-S39, ESI) for the **1d** series substituted at the C6 position led to the same conclusions as for **1a** (*vide supra*). Inductive electronic (-I) effects dominate for F and OCF_3 , while

resonance effects (+M) are the key for NMe_2 . For OCH_3 , inductive and mesomeric (+M, $\sigma_p = -0.27$) effects can be suggested. Consequently, bands I, II and III are significantly modified with the two π electron-donating substituents (OCH_3 and NMe_2 , ICT character), but only slightly tuned by the fluorinated groups (F and OCF_3).

By considering the influence of the substitution pattern at the C7 position (Table S11, Figure S11, ESI) in the **1d** series (F: **2e**, OCF_3 : **3d**, OCH_3 : **4e**, NMe_2 : **5c**), one observes an obvious effect of the F and OCF_3 substitution with hypsochromic and bathochromic shifts of the $^1\text{L}_a$ and $^1\text{L}_b$ transitions, respectively (*vide supra*). For NMe_2 , the $^1\text{L}_a$ band is bathochromically shifted to 405 nm ($\epsilon^{405} = 3.03 \times 10^3\text{ M}^{-1}\text{ cm}^{-1}$), with also a significant red shift of band III. By contrast with the 6-substituted analogue **4d**, no absorption in the visible region is observed for the OCH_3 substitution at the C7 position **4e**. The common feature for **4d** and **4e** derivatives is the strong bathochromic shifts of their respective $^1\text{L}_b$ transitions. ^{13}C NMR studies (Table S9, Figure S9, Figure S35 and Figures S40-S43, ESI) revealed the expected strong deshielding of the C7 signal with concomitant shielding of the C6 and C8 signals, the shielding of the C6 signal being larger for the NMe_2 substitution than for its OCH_3 counterpart. For the electron-donating NMe_2 substituent, a significant ICT character can be suggested by the shielding of the C3 signal borne by the pyridyl ring.

Emission properties. To get further insights into the auxochromic effects, we recorded the emission spectra of the compounds considered in this work. More precisely, upon excitation on the $\pi\text{-}\pi^*$ transitions ($\lambda_{\text{exc}} = 314 - 322\text{ nm}$, $A^{\lambda_{\text{exc}}} \leq 0.1$), the emission spectra of the C2- and C4-substituted quinolines were measured (Figure S12, ESI). These compounds are characterized by very weak emission signals with maxima ranging from 360 to 425 nm close to that of the parent quinoline.^[31] As already observed above, the introduction of fluorinated units on the pyridyl ring has a little impact on the emission properties of the quinoline unit. Furthermore, substitution by fluorine (**1a** series, Figure S13, ESI) or trifluoromethoxy (**1d** series, Figure S14, ESI) on the phenyl ring at the C6 and C7 positions has also a weak influence on the position, shape and intensity of the quinoline-centered emission. By contrast, substitution at the C8 position by fluorine drastically increases the intensity of the emission of the quinoline moiety, and simultaneously shifts it by *ca.* 20 nm (Figure S13, ESI). The corresponding compound **2c** strongly fluoresces compared to the "best" quinolines of our series (Table 1). This indicates that the observed quinoline-centered emission originates from the $\text{S}_1 \rightarrow \text{S}_0$ radiative deactivation and is related to the $^1\text{L}_a$ absorption, that is, respects the Kasha's rule.^[32] Substitution at the C8 position with other groups (*e.g.*, CH_3), has also a clear impact on the quinoline emission profile (Figures S15 and S16, ESI).

We next turned our attention to the effect of methoxy and dimethylamino groups on the emission of the fluorinated quinolines **1a** and **1d**. Substitution by OCH_3 group (-I and +M directing group) at the phenyl ring (C6 and C7, **1a** and **1d**

ARTICLE

Journal Name

series) markedly increases the intensity of the emission band of the quinoline unit without affecting its position (Table 1, Figures S17 and S18, ESI). By contrast, substitution of the C6 and C7 position by NMe₂ drastically alters both the intensity (significant increase with respect to either **1a** or **1d** parent quinolines, Figures S19 and S20, ESI) as well as the position (bathochromic shifts of *ca.* 100 nm with respect to the methoxy substitution), (Table 1).

Table 1. Emission properties in 1,2-dichloroethane of the substituted quinoline derivatives.^a

Compound		λ_{em} (nm)	$Q^{rel} = A_d/A_r$
Rf ¹ = CF ₃	1a	361	0.008
Rf ¹ = CHF ₂	1d	360	nd
Rf ¹ = CF ₃ , 6-F	2a	355	0.010
Rf ¹ = CF ₃ , 7-F	2b	361	0.014
Rf ¹ = CF ₃ , 8-F	2c	381	0.399
Rf ¹ = CHF ₂ , 6-OCF ₃	3c	383	0.013
Rf ¹ = CHF ₂ , 7-OCF ₃	3d	364	0.006
Rf ¹ = CHF ₂ , 8-OCF ₃	3e	381	0.024
Rf ¹ = CHF ₂ , 7-F, 8-CH ₃	6b	375	0.032
Rf ¹ = CHF ₂ , 7-Cl, 8-CH ₃	7b	373	0.010
Rf ¹ = CF ₃ , 7-F, 8-CH ₃	6a	381	0.025
Rf ¹ = CF ₃ , 7-Cl, 8-CH ₃	7a	405	nd
Rf ¹ = CF ₃ , 6-OCH ₃	4a	383	0.264
Rf ¹ = CF ₃ , 7-OCH ₃	4b	390	0.099
Rf ¹ = CF ₃ , 8-OCH ₃	4c	439	1.000
Rf ¹ = CHF ₂ , 6-OCH ₃	4d	381	0.215
Rf ¹ = CHF ₂ , 7-OCH ₃	4e	385	0.104
Rf ¹ = CHF ₂ , 8-OCH ₃	4f	435	0.926
Rf ¹ = CF ₃ , 6-NMe ₂	5a	478	0.620
Rf ¹ = CHF ₂ , 6-NMe ₂	5b	474	0.562
Rf ¹ = CHF ₂ , 7-NMe ₂	5c	492	0.265

^aSolvent: 1,2-dichloroethane, $T = 25.0(2) ^\circ\text{C}$. See Scheme 1 for the chemical structures of the defined quinolines. Q^{rel} stands for relative fluorescent quantum yield with respect to the most emissive derivative, namely **4c**. For all the compounds: emission and excitation band widths = 15 and 20 nm, respectively; band-pass filter at 290 nm; 1% attenuator and $\lambda_{exc} = 300$ nm.

This is consistent with the UV-vis. absorption results: substituents with strong mesomeric character drastically tune both the absorption and the emission properties in rather similar fashions. By contrast, strong inductive electron-withdrawing groups (F, OCF₃) have much less impact on the spectroscopic properties of the quinolines. The OCH₃ occupies an intermediate spot due to its mesomer (+M) and inductive (-I) electronic effects. The C6-substitution by OCH₃ systematically led to compounds that fluoresce more strongly with respect to the C7-substituted analogues (Table 1).

Similarly to substitution at the C8 position by F or OCF₃, a significant increase of the emission signal concomitant with a bathochromic shift of 50-60 nm was observed upon C8-substitution with a methoxy group. The red shifts that were measured are much larger than with fluorine or trifluoromethoxy moieties. As a consequence, the S₁→S₀ emission of **4c** and **4f** is shifted to *ca.* 430-440 nm (Table 1). We noted, that steric interactions are probably a dominating factor for the C8-substitution as shown by the marked alterations of the quinoline emission (*i.e.*, red shifts and enhancement) upon methyl substitution (*e.g.*, **6a**, **7a**, **6b**, **7b**,

Table 1) or monofluorination (*e.g.*, **2c**). Figure 8 summarizes in relative terms the effects of the substitution pattern at the C6-position (Figure S21, ESI for **1a** series, C7-position and Figures S22-S23, ESI for **1d** series, C6- and C7-positions).

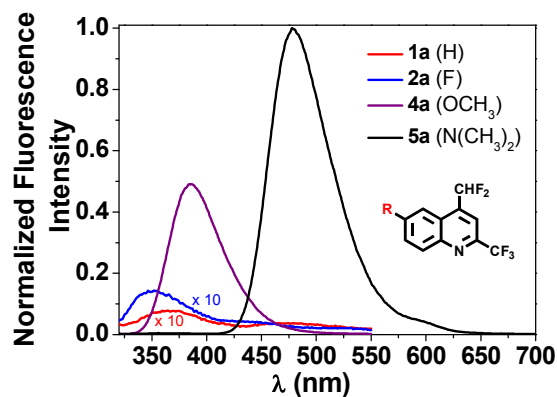


Figure 8. Influence on the emission spectra of the substitution on the C6 position for quinoline derivatives bearing a CF₃ in C2 and a CHF₂ in C4 (derivative **1a** as a scaffold reference). Solvent: 1,2-dichloroethane, $T = 25.0(2) ^\circ\text{C}$. Emission and excitation band widths = 15 and 20 nm; band-pass filter at 290 nm; 1% attenuator. The emission intensities have been normalized with respect to the absorbances of the quinoline solutions and therefore reflect the relative quantum yields. The absorbances at excitation wavelength are always below 0.1 to prevent inner filter effects.

Electrochemical properties. We next describe in this section the electrochemical properties (Table 2) of the fluorinated quinoline derivatives (Scheme 1) focusing mainly on the **1d** series to assess the influence of the substitution pattern at the benzene- and/or pyridyl-type rings. All compounds exhibit two well-defined cathodic peaks in the potential range from -1.4 V to -2.4 V with, in most cases, no evidence for anodic peaks (Figure 9A, Figures S24-S29, ESI). The repetitive scans were found to be fairly reproducible suggesting the absence of adsorption processes or degradation products under these experimental conditions. In aprotic medium, these two well-defined reduction steps likely correspond to the successive formation of the monoradical-anion (1st step) and the dianion (2nd step), respectively. This is in line with literature data based on related quinolines investigated in aprotic solvents such as DMF.^[33] The marked difference with data in DMF is based on the fact that the 1st step is a reversible one-electron transfer, while the 2nd is an irreversible one-electron process. Under our experimental conditions, the two cathodic signals were assigned to irreversible one-electron transfers as evidenced by the absence of a current signal in the reverse scan as well as the linear dependence of the cathodic potentials as a function of the scan rate (Figure 9B). Furthermore, the linear dependence of the peak current (i_{pc}) of the two cathodic signals of **1d** on the square root of the sweep rate ($v^{0.5}$) (Figure 9C) indicates a diffusion controlled electron process. Therefore, the substituted quinolines based on **1d** participate to electrode reaction as diffusional species. In aprotic solvents such as 1,2-dichloroethane, the fluorinated quinolines reduction thus occurs *via* two successive one-electron

transfers. The monoradical-anion is formed in the E_{pc1} reduction step, and is then reduced to its related dihydroquinoline dianion in a second E_{pc2} step (Figure 9A). The quinolines considered in this work are not subject to any inter- or intramolecular proton transfers and therefore the electrochemical properties are strictly associated to the successive formation of the two anionic reduced species (Figure 9). In addition, an important property of the fluorinated quinolines of the **1d** series is a broad potential range of redox inertness. Indeed, no redox reaction occurs for potential values ranging from +2.5 V to \sim -1.3 V.

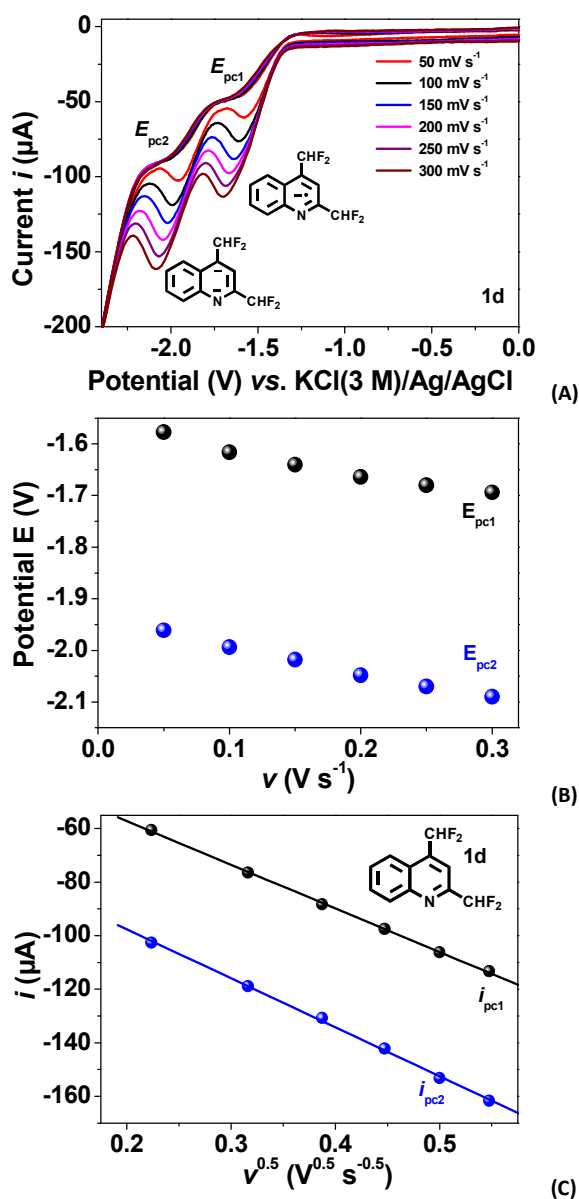


Figure 9. (A) Cyclic voltammograms of **1d** (\sim mM) as a function of the sweep rate. (B) Variation of the cathodic potentials as a function of the sweep rate demonstrating the irreversible character of the two successive one-electron transfers. (C) Variation of the cathodic current intensities as a function of the square root of the scan rate indicating diffusion controlled redox processes. Solvent: 1,2-dichloroethane; $T = 25.0(2)^\circ\text{C}$; $I = 0.1\text{ M}$ (NBu_4BF_4);

reference electrode = KCl (3 M)/ Ag/AgCl ; working electrode = glassy carbon disk of 0.07 cm^2 area.

A clear relationship (Figure 10) can be observed between the reduction potentials of the first (E_{pc1}) and second (E_{pc2}) electrochemical processes. This suggests that the substituents borne by the quinoline **1d** induce the same electronic effects on the parent unit and its 1-electron reduced counterpart.

Comparison of cyclic voltammograms of the **1a** and **1d** quinolines (Figure S24, ESI) shows that the two-successive irreversible one-electron transfers are preserved irrespective of the pyridyl-ring substitution pattern. A significant anodic shift of the first reduction peak of $\text{ca. } 120\text{ mV}$ can be observed on substitution of the C2- CHF_2 group by a CF_3 , while both the position and shape of the second reduction peak are seemingly unaffected. This agrees with the stronger inductive electron-withdrawing effect of CF_3 ($\sigma_m = +0.43$, $\sigma_p = +0.54$) compared to CHF_2 ($\sigma_m = +0.29$, $\sigma_p = +0.32$) and suggests that the separation between the two reduction waves are intrinsically dependent on the pyridyl-ring substitution.

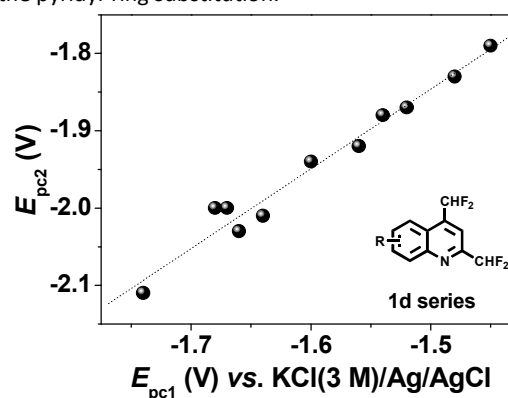


Figure 10. Variation of E_{pc2} (V, second cathodic step) as a function of E_{pc1} (V, first cathodic step). Solvent: 1,2-dichloroethane; $T = 25.0(2)^\circ\text{C}$; $I = 0.1\text{ M}$ (NBu_4BF_4); $v = 200\text{ mV s}^{-1}$; reference electrode = KCl (3 M)/ Ag/AgCl ; working electrode = glassy carbon disk of 0.07 cm^2 area; auxiliary electrode = Pt wire. The dashed line is only provided as a guide for the eyes.

Table 2. Electrochemical data (1st and 2nd reduction processes) measured using cyclic voltammetry (CV) for all the substituted quinolines of the **1d** series.^a

Compound	E_{pc1} (V)	E_{pc2} (V)	$E_{pc1}-E_{pc2}$ (V)	
$\text{Rf}^1 = \text{CF}_3$	1a	-1.52	-2.00	0.48
$\text{Rf}^1 = \text{CHF}_2$	1d	-1.64	-2.01	0.37
$\text{Rf}^1 = \text{CHF}_2$, 6-F	2d	-1.56	-1.92	0.36
$\text{Rf}^1 = \text{CHF}_2$, 7-F	2e	-1.52	-1.87	0.35
$\text{Rf}^1 = \text{CHF}_2$, 6-OCF ₃	3c	-1.48	-1.83	0.35
$\text{Rf}^1 = \text{CHF}_2$, 7-OCF ₃	3d	-1.45	-1.79	0.34
$\text{Rf}^1 = \text{CHF}_2$, 6-OCH ₃	4d	-1.67	-2.00	0.33
$\text{Rf}^1 = \text{CHF}_2$, 7-OCH ₃	4e	-1.66	-2.03	0.37
$\text{Rf}^1 = \text{CHF}_2$, 6-NMe ₂	5b	-1.74	-2.11	0.37
$\text{Rf}^1 = \text{CHF}_2$, 7-NMe ₂	5c	-1.68	-2.00	0.32
$\text{Rf}^1 = \text{CHF}_2$, 7-F, 8-CH ₃	6b	-1.60	-1.94	0.34
$\text{Rf}^1 = \text{CHF}_2$, 7-Cl, 8-CH ₃	7b	-1.54	-1.88	0.34

^a Solvent: 1,2-dichloroethane; $T = 25.0(2)^\circ\text{C}$; $I = 0.1\text{ M}$ (NBu_4BF_4); $v = 200\text{ mV s}^{-1}$; reference electrode = KCl (3 M)/ Ag/AgCl ; working electrode = glassy carbon disk of 0.07 cm^2 area; auxiliary electrode = Pt wire. See Scheme 1 for the chemical

ARTICLE

Journal Name

structures of the defined quinolines.

Let us now discuss the first one-electron process associated to the E_{pc1} values. By considering the presence of the fluorine substitution on the benzene-type ring (Figure S25, ESI), one clearly observes that the first (and second) reduction peak is anodically shifted of 80 mV (**2d**, fluorine at the C6-position) and 120 mV (**2e**, fluorine at the C7 position). This indicates that the fluorine-based quinolines are more prone to reduction than the parent quinoline **1d**. Therefore, the F-substituent with electron-withdrawing capacities ($\sigma_m = +0.34$ and $\sigma_p = +0.06$) decreases the electronic density of the electroactive quinoline **1d** unit and facilitates the reduction of the corresponding compounds. This effect is even more marked for F-substitution at the C7 position than at the C6 position as evidenced by the further *ca.* 40 mV anodic shift of the first cathodic signal. These observations are in agreement with the absorption and emission data and confirm that F substitution has mainly an electron-withdrawing inductive effect in the present series. The introduction of the methyl substituent at the C8-position (**6b** and **7b**) confers to the corresponding systems less oxidant properties due to the inductive donor properties of the CH_3 group.

On the other hand, it has been reported that the electrochemical reduction process of aryl halogenides may lead to the cleavage of the C-halogen bond along the formation of the monoradical-anion intermediate.^[34] For fluoro-substituted azaaromatics such as quinoline, the stability of the monoradical-anions was found to be higher than that of comparable fluoro-substituted arenes preventing defluorination pathways.^[33b, 34] For **2d**, **2e**, **6b** or **7b** (Figure S29, ESI), we underline that no dehalogenation was observed. For the OCF_3 substitution, the larger electron-withdrawing properties ($\sigma_m = +0.38$ and $\sigma_p = +0.35$) compared to F lead to the most oxidant compounds of the **1d** series (Table 2). Additionally, the CV voltammograms of both **3c** and **3d** exhibit a third irreversible reduction peak at *ca.* -2.2V as well as an irreversible oxidation peak at +1.32 V and +1.36 V, respectively (Figure S26, ESI). We tentatively associate those to the dissociation of the $\cdot\text{CF}_3$ radical leading to a phenolic unit that can give rise to an oxidation signal. No such behaviour was observed for OCH_3 substitution (Figure S27, ESI). As suggested by the analysis of the optical spectra, the OCH_3 substituent can act either as an electron-withdrawing unit or a mesomer electron-donating group. As a consequence, the substitution by OCH_3 either at the C6 or C7 positions has a weak effect on the electrochemical properties.

The NMe_2 substitution at the C6 or C7 position of **1d** led to the largest cathodic shift of the two successive reduction peaks (Figure S28, ESI). This agrees very well with the electron-donating capacities of this group. A cathodic shift of *ca.* 100 mV (+40 mV) was observed for the C6 (C7) substitution.

The reactivity of the electroactive monoradical anion intermediates mainly depends on the quinoline electronic properties, *i.e.*, the potentials of the first reduction wave can be related to the electron affinities of the molecule, which can

be rationalized by the Hammett^[27a)] σ constants (Figure 11 and the above discussions).

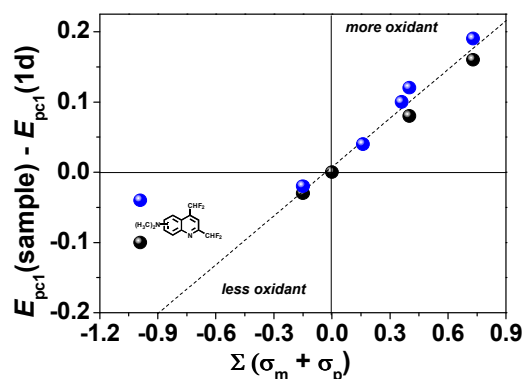


Figure 11. Plot of ΔE_{pc1} ($E_{pc1(\text{sample})} - E_{pc1(\mathbf{1d})}$) vs. $\Sigma(\sigma_m + \sigma_p)$ for the substituted fluorinated quinolines of the **1d** series (black circles: C6-substituted; blue circles: C7-substituted). Solvent: 1,2-dichloroethane; $l = 0.1$ M (NBu_4BF_4); $T = 25^\circ\text{C}$; $\nu = 200$ mV s^{-1} ; reference electrode = $\text{KCl}(3 \text{ M})/\text{Ag}/\text{AgCl}$; working electrode = glassy carbon disk of 0.07 cm^2 area. σ_m stands for a *meta*-substituted group with respect to the reactive centre and σ_p designates a *para*-substituted function. In this approach, we used the sum ($\sigma_m + \sigma_p$) to describe the electronic effect of a substituent on the electroactive quinoline core.

Figure 11 illustrates the variation of ΔE_{pc1} for the first irreversible electron transfer. A clear linear relationship between ΔE_{pc1} and the nature of the electronic substituent ($\Sigma(\sigma_m + \sigma_p)$) can be observed. This suggests that the quinoline unit is solely influenced by inductive or mesomeric electronic effects irrespective of the position of the substitution (C6, C7 or C8) on the benzene-type ring. Electron-withdrawing substituents decrease the electronic density of the quinoline unit and render these compounds “more oxidant”, while electron-donating substituents increases the electronic density and thereby decreases the propensity of the corresponding redox compounds to be reduced. With the exception of the dimethylamino substitution, the intercept at the origin is close to zero (Figure 11) indicating that the electron transfers are not complicated by coupled chemical reactions such as proton transfer or complexes formation (dimerization, oligomerization...). Deviation from such a linear relationship, however, occurs for the dimethylamino function substituted at the C6 or C7 positions. This might result in a limited conjugation of the dimethylamino group with the quinoline unit, therefore limiting the cathodic shifts of the reduction potentials. These data agree with those derived from the spectrophotometric absorption and ^{13}C studies.

TD-DFT calculations. We have finally performed TD-DFT calculation to obtain complementary insights into the low-lying excited-states of the synthesized molecules. Experimentally, very similar optical spectra were obtained in the **1a-1e** series (Figure S3 in the ESI). For **1a**, **1b**, **1c**, **1d** and **1e** we compute a vertical transition wavelength of 322 nm, 328 nm, 324 nm, 312 nm and 318 nm, all values that are close from one another as well as to experiment (Table S1 in the ESI). These similarities in

the **1a-1e** series are consistent with alike ICT characters. Indeed, we computed very similar ICT distances ($1.83 \pm 0.04 \text{ \AA}$) in that series, values that can be viewed as relatively mild. In Figure 12, we show density difference plots for **1a** and **1c**. The excited-state topologies are similar, with an ICT from the phenyl (mostly in blue) to the pyridyl (mostly in red) rings, the two-carbon bearing the CF_3 and/or CHF_2 substituents acting as acceptors, as expected. Substitution at C6 has a minor impact on the first band experimentally (*e.g.*, see Table S2 in the ESI), and we indeed computed for **2a**, a vertical excitation at 315 nm, very close to the one of **1a**. As can be seen in Figure 12, the additional fluorine atom acts as a trifling secondary π -donor for the first band, but does not significantly perturb the topology of the excited-state, confirming that the main impact of F is -I. At C7 (**2b**), the fluorine atom induces a small bathochromic shift (324 nm) compared to **1a**, which is qualitatively in line with experiment, but this does not change the shape of the excited-state significantly (Figure 12). In any case, these effects are rather small and have a negligible impact on the computed ICT distance that remains similar to the one obtained for **1a**. Much larger changes are found when adding strong donor groups at C6, as TD-DFT returns the lowest band at 359 nm in **4a** and 427 nm in **5a**. These large bathochromic shifts are in line with experiment with maxima at 340 and 406 nm, respectively (see Figure 6). As can be seen in Figure 12, when adding a methoxy group, the ICT character of the state increases, the oxygen playing a significant role; the ICT distance attaining 2.17 \AA according to our calculations. The use of a dimethylamino donor group has an even stronger impact on the topology of the excited-state and further increases the ICT distance up to 2.32 \AA .

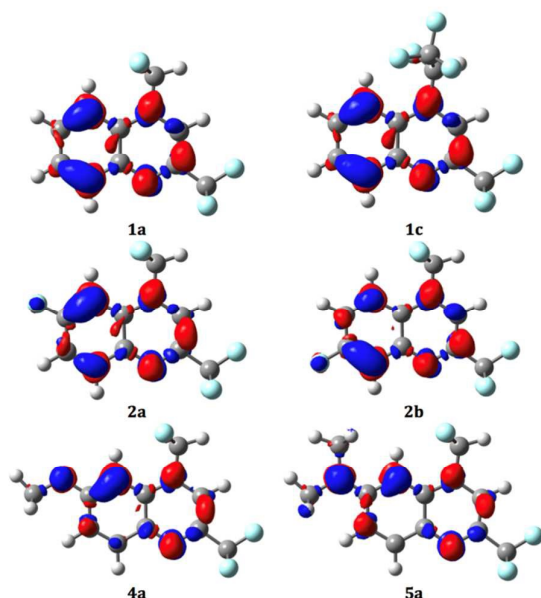


Figure 12. Density difference plots between the lowest excited-state and the ground-state for selected compounds. The blue (red) regions indicate decrease (increase) of electronic density upon excitation. Contour threshold: 3×10^{-3} au.

Conclusions

Based on the advantageous use of FARs, a homogeneous series of unreported polyfunctionalized fluoroalkylated quinolines has been prepared. Their physico-chemical properties have been investigated by absorption and emission spectrophotometries, ^{13}C NMR spectroscopy, cyclic voltammetry and TD-DFT calculations. Regarding their absorption properties, substitution of positions C2 and C4 of the quinoline core by fluoroalkylated groups (CHF_2 , CHFCI , CF_3 or CHF_2CF_3) moderately affects both the $^1\text{L}_b$ (band I) and $^1\text{L}_a$ (band II) π - π^* transitions. The excited state topologies of the lowest state predicted by TD-DFT calculations were also found to be fairly similar. Due to the presence of fluoroalkylated substituents, ICT (ICT distances of *ca.* 1.83 \AA) was evidenced from the phenyl to the pyridyl rings, the C2 and C4 carbons acting as acceptors. Substitution by fluorinated (F or OCF_3) groups at the C6, C7 or C8 positions induced minor changes of the absorption band of the quinoline reflecting alike ICT character. The fluorine atom at the C7 was, however, shown to act as a very weak secondary π -electron donor, but without significant alteration of the excited state topology. The OCH_3 and NMe_2 substituents, that display strong mesomeric effects, stood in interesting contrast and led to marked alterations of the absorption properties of the quinoline. Band III experienced strong bathochromic and hypochromic shifts concomitant to alterations of the shape and position of bands I and II. For the NMe_2 derivative, a broad and intense absorption emerges in the visible region. These features are consistent with an increase of the ICT character of the low lying excited states (computed ICT distances of 2.17 and 2.32 \AA for OCH_3 and NMe_2 , respectively). ^{13}C NMR data further support these findings. Indeed, F and OCF_3 substitutions mainly influence the neighbouring carbons, whereas for derivatives bearing OCH_3 and NMe_2 substitutions, the shielding of the C2 and C4 ^{13}C signals confirm a resonance process along the whole aromatic system and thus excited states with increased ICT character.

The substituents electronic effects were also probed by spectrofluorimetry. Introduction of fluorinated groups has a little influence on the emission profile of the quinoline unit (*i.e.*, very weak emission signals with close maxima). Steric interaction induced by C8 substitution (F, OCF_3 or CH_3), however, drastically increases the emission intensity. As a consequence, compound **2c** with C8-F substitution fluoresces more strongly than the "best" quinolines of our series. Substitution by OCH_3 also markedly increases the intensity of the emission band of the quinoline unit, though without affecting its position, while substitution by NMe_2 drastically alters both the intensity and the position. Substituents with strong mesomeric character drastically tune both the absorption and the emission properties in similar fashions. Groups having predominantly inductive electron-withdrawing properties (F, OCF_3) have much less impact on the

ARTICLE

Journal Name

spectroscopic properties of the quinolines. The OCH₃ stands occupying an intermediate spot due to its mesomer (+M) and inductive (-I) electronic effects.

With respect to their electrochemical properties, all the compounds exhibit two well-defined cathodic responses in the -1.4 V / -2.4 V range with no evidence for anodic peaks. Importantly, these fluorinated quinolines were found to be characterized by redox inertness over a broad potential range (from +2.5 V to *ca.* -1.3 V) in line with the harshness of reaction conditions used to further chemically functionalize these compounds. The clear relationship found between the reduction potentials of the first (E_{pc1}) and second (E_{pc2}) electrochemical processes suggests that the phenyl substitution pattern induces the same electronic effects on the parent unit and its 1-electron reduced counterpart. The potential $E_{pc1} - E_{pc2}$ separation was, however, found to be intrinsically dependent on the pyridyl-ring substitution pattern as evidenced by the anodic shift (*ca.* 120 mV) of only the first reduction peak when going from a C2-CHF₂ to a C2-CF₃ substitution. Further substitution with electron-withdrawing fluorine-containing groups decreases the electronic density of the electroactive quinoline and facilitates the reduction of the corresponding compounds. The most oxidant system is indeed reached with OCF₃ substitution. By contrast, NMe₂ substitution leads to the largest cathodic shift of the two successive reduction peaks in line with the electron-donating capacities of this group.

The present extensive physico-chemical study allowed getting deeper insights into the electronic properties of these polyfunctionalized fluoroalkylated quinolines. By fine-tuning the substitution of the quinoline pattern (easily feasible by the developed synthetic methodologies), valuable properties (*i.e.*, electrochemical, spectroscopic, inertness/robustness) can be conferred to this compound, which opens the way to targeted design in several areas such as fluorescent and robust quinolines for medicinal chemistry and bio-imaging.

Experimental Section

Solvents and Materials. The fluorine-enriched derivatives 1-7 were synthesized according to literature procedures.^[19] The electrochemical and spectrophotometric (absorption and emission) properties of the substituted quinoline derivatives were examined in spectroscopic grade 1,2-dichloroethane (Carlo Erba, 99.8% for spectroscopy). All the stock solutions were prepared by weighting solid products using a Mettler Toledo XA105 Dual Range (0.01/0.1 mg - 41/120 g). The complete dissolution of the ligands was obtained with the help of ultrasonic bath (Bandelin Sonorex RK102). All the physico-chemical measurements were carried out at 25.0(2) °C.

Absorption studies. The UV-visible absorption spectra were recorded from 220 to 800 nm with an Agilent Cary 5000 spectrophotometer maintained at 25.0(2) °C by the flow of a Cary Varian Dual Cell Peltier accessory. Quartz optical cells with pathlength of 1 cm were used for these measurements.

Emission studies. The fluorescence emission spectra were recorded from 300 to 800 nm on a Perkin-Elmer LS-50B maintained at 25.0(2) °C by the flow of a Haake FJ thermostat. The light source was a pulsed xenon flash lamp with a pulse width at half-peak height <10 μs and power equivalent to 20 kW. The slit width was adjusted for both excitation and emission to reach the maximum of intensity. The spectrofluorimetric signal of the emission were measured at absorbances <0.1 to minimize reabsorption processes.

Electrochemistry. The redox potentials of the fluorinated quinoline derivatives were measured by cyclic voltammetry (CV) at 25 °C in 1,2-dichloroethane solvent. Cyclic voltammetry of the quinolines (~ mM solutions) was carried out using a Voltalab 50 potentiostat/galvanostat (Radiometer Analytical MDE15 polarographic stand, PST050 analytical voltammetry and CTV101 speed control unit) controlled by the Voltmaster 4 electrochemical software. A conventional three-electrode cell (10 mL) was employed in our experiments with a glassy carbon disk (GC, $s = 0.07 \text{ cm}^2$) set into a Teflon rotating tube as a working electrode, a Pt wire as a counter electrode, and KCl (3 M)/Ag/AgCl reference electrode (+210 mV vs NHE).^[22] Prior to each measurement, the surface of the GC electrode was carefully polished with 0.3 μm aluminium oxide suspension (Escil) on a silicon carbide abrasive sheet of grit 800/2400. Thereafter, the GC electrode was copiously washed with water and dried with paper towel and argon. The electrode was installed into the voltammetry cell along with a platinum wire counter electrode and the reference. The solutions containing *ca.* 10⁻³ M of the quinoline derivatives were vigorously stirred and purged with O₂-free (Sigma Oxiclear cartridge) argon for 15 minutes before the voltammetry experiment was initiated, and maintained under an argon atmosphere during the measurement procedure. The voltammograms (cyclic voltammograms - CV) were recorded at room temperature (23(1)°C) in 1,2-dichloroethane with 100 mM tetra-*n*-butylammonium tetrafluoroborate (Alfa Aesar, +99%) as supporting and inert electrolyte.^[23a, 35] The voltage sweep rate was varied from 50 to 300 mV s⁻¹ and several cyclic voltammograms were recorded from +2.5 V to -2.5 V. Peak potentials were measured at a scan rate of 200 mV s⁻¹ unless otherwise indicated. Redox potentials were determined from oxidation and reduction potentials.

DFT calculations. All calculations have been made with the Gaussian16 program,^[36] with the B3LYP exchange-correlation functional using the 6-311++G(d,p) atomic basis set for the ground-state properties and the 6-311++G(2d,p) atomic basis set for the excited-state properties. We have applied the *ultrafine* integration grid for all calculations and used default convergence thresholds but for a tightened SCF convergence (at least 10⁻⁸ au) and geometry optimization (10⁻⁵ au on rms forces) thresholds. Our calculations have been made in three steps: i) geometry optimizations of the ground-state structure without imposing symmetry constraints; ii) frequency calculation to confirm that the structures are true minima of the potential energy surface; and iii) TD-DFT calculations of the

electronic excited-states. For all steps, we used the Polarizable Continuum Model (PCM) approach to model solvation effects (here 1,2-dichloroethane) using the corrected linear-response approach^[37] in its *non-equilibrium* limit for the TD-DFT part. Intramolecular charge-transfer parameters (distances) have been computed using Le Bahers's method.^[38]

Conflicts of interest

There are no conflicts to declare

Acknowledgements

We thank the Centre National de la Recherche Scientifique (CNRS) and the University of Strasbourg (UMR 7042-LIMA) and are very much grateful to Bayer S.A.S. for a grant to F.A.. The French Fluorine Network (GIS Fluor) is also acknowledged. The authors are grateful to Matthieu Chessé for fluorescence data acquisition. This work used computational resources of the CCIPL Waves cluster installed in Nantes thanks to the support of the *Région des Pays de la Loire*.

Notes and references

- a) K. Suresh, B. Sandhya and G. Himanshu, *Mini-Rev. Med. Chem.*, 2009, **9**, 1648-1654; b) K. D. Thomas, A. V. Adhikari, S. Telkar, I. H. Chowdhury, R. Mahmood, N. K. Pal, G. Row and E. Sumesh, *Eur. J. Med. Chem.*, 2011, **46**, 5283-5292; c) K. Kaur, M. Jain, R. P. Reddy and R. Jain, *Eur. J. Med. Chem.*, 2010, **45**, 3245-3264; d) S. R. Patel, R. Gangwal, A. T. Sangamwar and R. Jain, *Eur. J. Med. Chem.*, 2015, **93**, 511-522; e) O. Afzal, S. Kumar, M. R. Haider, M. R. Ali, R. Kumar, M. Jaggi and S. Bawa, *Eur. J. Med. Chem.*, 2015, **97**, 871-910; f) C.-H. Tseng, C.-C. Tzeng, C.-C. Chiu, C.-Y. Hsu, C.-K. Chou and Y.-L. Chen, *Bioorg. Med. Chem.*, 2015, **23**, 141-148; g) X. Lv, H. Ying, X. Ma, N. Qiu, P. Wu, B. Yang and Y. Hu, *Eur. J. Med. Chem.*, 2015, **99**, 36-50; h) W. Liao, G. Hu, Z. Guo, D. Sun, L. Zhang, Y. Bu, Y. Li, Y. Liu and P. Gong, *Bioorg. Med. Chem.*, 2015, **23**, 4410-4422; i) A. Kamal, A. Rahim, S. Riyaz, Y. Poornachandra, M. Balakrishna, C. G. Kumar, S. M. A. Hussaini, B. Sridhar and P. K. Machiraju, *Org. Biomol. Chem.*, 2015, **13**, 1347-1357.
- a) I. E. Wheeler, D. W. Hollomon, G. Gustafson, J. C. Mitchell, C. Longhurst, Z. Zhang and S. J. Gurr, *Mol. Plant Pathol.*, 2003, **4**, 177-186; b) J. Jampilek, R. Musiol, M. Pesko, K. Kralova, M. Vejsova, J. Carroll, A. Coffey, J. Finster, D. Tabak, H. Niedbala, V. Kozik, J. Polanski, J. Csollei and J. Dohnal, *Molecules*, 2009, **14**, 1145-1159; c) J. Mulero, G. Martinez, J. Oliva, S. Cermenon, J. M. Cayuela, P. Zafrilla, A. Martinez-Cacha and A. Barba, *Food Chem.*, 2015, **180**, 25-31.
- a) S. Karthik, B. Saha, S. K. Ghosh and N. D. Pradeep Singh, *Chem. Commun.*, 2013, **49**, 10471-10473; b) S. A. Jenekhe, L. Lu and M. M. Alam, *Macromolecules*, 2001, **34**, 7315-7324; c) V. Bhalla, V. Vij, M. Kumar, P. R. Sharma and T. Kaur, *Org. Lett.*, 2012, **14**, 1012-1015; d) S. Halder, S. Dey and P. Roy, *RSC Adv.*, 2015, **5**, 54873-54881; e) Y. W. Choi, J. J. Lee and C. Kim, *RSC Adv.*, 2015, **5**, 60796-60803; f) M. Tomar, A. Z. Ashar, K. S. Narayan, K. Müllen and J. Jacob, *J. Polym. Res.*, 2016, **23**, 50.
- Z. H. Skraup, *Ber. Dtsch. Chem. Ges.*, 1880, **13**, 2086-2087.
- a) O. Doebner and W. V. Miller, *Ber. Dtsch. Chem. Ges.*, 1881, **14**, 2812-2817; b) V. Y. Denisov, T. N. Grishchenkova, T. B. Tkachenko and S. V. Luzgarev, *Russ. J. Org. Chem.*, 2016, **52**, 1797-1803; c) Y.-C. Wu, L. Liu, H.-J. Li, D. Wang and Y.-J. Chen, *J. Org. Chem.*, 2006, **71**, 6592-6595; d) S. E. Denmark and S. Venkatraman, *J. Org. Chem.*, 2006, **71**, 1668-1676; e) S. A. Yamashkin and E. A. Oreshkina, *Chem. Heterocycl. Compd.*, 2006, **42**, 701-718.
- M. Conrad and L. Limpach, *Ber. Dtsch. Chem. Ges.*, 1887, **20**, 944-948.
- P. Friedlaender, *Ber. Dtsch. Chem. Ges.*, 1882, **15**, 2572-2575.
- a) W. Pfitzinger, *J. Prakt. Chem.*, 1886, **33**, 100-100; b) W. Pfitzinger, *J. Prakt. Chem.*, 1888, **38**, 582-584.
- A. Combes, *Bull. Soc. Chim. Fr.*, 1888, **49**, 89-92.
- a) O. Meth-Cohn, B. Narine and B. Tarnowski, *J. Chem. Soc., Perkin Trans. 1*, 1981, 1520-1530; b) O. Meth-Cohn, *Heterocycles*, 1993, **35**, 539-557.
- a) K. T. Finley, in *Kirk-Othmer Encyclopedia of Chemical Technology*, John Wiley & Sons, Inc., 2000, p. 32; b) A. L. Zografos, in *Heterocyclic Chemistry in Drug Discovery* (Ed.: J. J. Li), John Wiley & Sons, Inc., 2013, pp. 471-534; c) J. J. Li, in *A Collection of Detailed Mechanisms and Synthetic Applications*, 3th ed., Springer-Verlag Berlin Heidelberg, 2006, p. 670.
- a) J. B. Bharate, R. A. Vishwakarma and S. B. Bharate, *RSC Adv.*, 2015, **5**, 42020-42053; b) G. Ramann and B. Cowen, *Molecules*, 2016, **21**, 986.
- a) Q. Zheng, P. Luo, Y. Lin, W. Chen, X. Liu, Y. Zhang and Q. Ding, *Org. Biomol. Chem.*, 2015, **13**, 4657-4660; b) J. Zheng, Z. Li, L. Huang, W. Wu, J. Li and H. Jiang, *Org. Lett.*, 2016, **18**, 3514-3517; c) R. I. Khusnutdinov, A. R. Bayguzina and U. M. Dzhemilev, *J. Organomet. Chem.*, 2014, **768**, 75-114; d) B.-C. Zhao, Q.-Z. Zhang, W.-Y. Zhou, H.-C. Tao and Z.-G. Li, *RSC Adv.*, 2013, **3**, 13106-13109; e) X. Zhou, Z. Qi, S. Yu, L. Kong, Y. Li, W. F. Tian and X. Li, *Adv. Synth. Catal.*, 2017, **359**, 1620-1625; f) Y. Liu, C. Wang, N. Lv, Z. Liu and Y. Zhang, *Adv. Synth. Catal.*, 2017, **359**, 1351-1358; g) S. Yu, Y. Li, X. Zhou, H. Wang, L. Kong and X. Li, *Org. Lett.*, 2016, **18**, 2812-2815.
- a) F. R. Leroux, B. Manteau, J. P. Vors and S. Pazenok, *Beilstein J. Org. Chem.*, 2008, **4**, 13; b) K. Uneyama, *Fundamentals in Organic Fluorine Chemistry*, Blackwell, Oxford, 2006; c) J.-P. Bégué and D. Bonnet-Delpon, *Bioorganic and Medicinal Chemistry of Fluorine*, John Wiley & Sons, Hoboken, New Jersey, 2008; d) G. Theodoridis, in *Advances in Fluorine Science*, Vol. 2 (Ed.: A. Tressaud), Elsevier B.V, 2006, pp. 120-175; e) S. Purser, P. R. Moore, S. Swallow and V. Gouverneur, *Chem. Soc. Rev.*, 2008, **37**, 320-330.
- a) G. Balz and G. Schiemann, *Ber. Dtsch. Chem. Ges.*, 1927, **60**, 1186-1190; b) P. Kirsch, *Modern Fluoroorganic Chemistry: Synthesis, Reactivity, Applications*, Wiley-VCH, Weinheim, Germany, 2004; c) V. Nenajdenko, in *Fluorine in Heterocyclic Chemistry Volume 2* (Ed.: V. Nenajdenko), Springer International Publishing, 2014, p. 768; d) S. D. Taylor, C. C. Kotoris and G. Hum, *Tetrahedron*, 1999, **55**, 12431-12477; e) R. D. Chambers, D. Holling, G. Sandford, A. S. Batsanov and J. A. K. Howard, *J. Fluorine Chem.*, 2004, **125**, 661-671.
- a) G. K. S. Prakash and A. K. Yudin, *Chem. Rev.*, 1997, **97**, 757-786; b) R. P. Singh and J. N. M. Shreeve, *Tetrahedron*, 2000, **56**, 7613-7632; c) Y. Kobayashi and I. Kumadaki, *Tetrahedron Lett.*, 1969, **10**, 4095-4096; d) T. Besset, T. Poisson and X. Pannecoucke, *Chem. Eur. J.*, 2014, **20**, 16830-16845.
- J. C. Sloop, C. L. Bumgardner and W. D. Loehle, *J. Fluorine Chem.*, 2002, **118**, 135-147.
- Y. Fujiwara, J. A. Dixon, R. A. Rodriguez, R. D. Baxter, D. D. Dixon, M. R. Collins, D. G. Blackmond and P. S. Baran, *J. Am. Chem. Soc.*, 2012, **134**, 1494-1497.
- F. Aribi, E. Schmitt, A. Panossian, J.-P. Vors, S. Pazenok and F. R. Leroux, *Org. Chem. Front.*, 2016, **3**, 1392-1415.

ARTICLE

Journal Name

- 20 a) B. Commare, E. Schmitt, F. Aribi, A. Panossian, J.-P. Vors, S. Pazenok and F. R. Leroux, *Molecules*, 2017, **22**, 977-1003; b) V. A. Petrov, S. Swearingen, W. Hong and W. Chris Petersen, *J. Fluorine Chem.*, 2001, **109**, 25-31; c) V. A. Petrov, *Adv. Org. Synth.*, 2006, **2**, 269-290; d) L. M. Grieco, G. A. Halliday, C. P. Junk, S. R. Lustig, W. J. Marshall and V. A. Petrov, *J. Fluorine Chem.*, 2011, **132**, 1198-1206; e) N. N. Yarovenko and M. A. Raksha, *Zh. Obshch. Khim.*, 1959, **29**, 2159-2163; f) N. N. Yarovenko and M. A. Raksha, *J. Gen. Chem. USSR (Engl. Transl.)*, 1959, **29**, 2125-2128; g) A. Takaoka, K. Iwamoto, T. Kitazume and N. Ishikawa, *J. Fluorine Chem.*, 1979, **14**, 421-428; h) S. Pazenok, N. Lui and A. Neeff, 2008, *WO 2008/022777*; i) F. Giornal, S. Pazenok, L. Rodefeld, N. Lui, J.-P. Vors and F. R. Leroux, *J. Fluorine Chem.*, 2013, **152**, 2-11; j) S. Pazenok, F. Giornal, G. Landelle, N. Lui, J.-P. Vors and F. R. Leroux, *Eur. J. Org. Chem.*, 2013, 4249-4253; k) S. Pazenok, N. Lui, A. Neeff, W. Etzel, J.-P. Vors, F. Leroux, G. Landelle and M. J. Ford, 2014, *WO 2014/187773*; l) E. Schmitt, G. Landelle, J.-P. Vors, N. Lui, S. Pazenok and F. R. Leroux, *Eur. J. Org. Chem.*, 2015, 6052-6060; m) S. Pazenok, N. Lui, C. Funke, W. Etzel and A. Neeff, 2015, *WO 2015/144578*; n) E. Schmitt, A. Panossian, J.-P. Vors, C. Funke, N. Lui, S. Pazenok and F. R. Leroux, *Chem. Eur. J.*, 2016, **22**, 11239-11244; o) F. Giornal, G. Landelle, N. Lui, J.-P. Vors, S. Pazenok and F. R. Leroux, *Org. Proc. Res. Dev.*, 2014, **18**, 1002-1009.
- 21 A. Vilsmeier and A. Haack, *Ber. Dtsch. Chem. Ges.*, 1927, **60**, 119-122.
- 22 J. R. Platt, *J. Chem. Phys.*, 1949, **17**, 484-495.
- 23 a) H. Baba and I. Yamazaki, *J. Mol. Spectrosc.*, 1972, **44**, 118-130; b) H. Takashi, *Bull. Chem. Soc. Jpn.*, 1963, **36**, 235-247.
- 24 T. C. F. Oliveira, L. F. V. Carmo, B. Murta, L. G. T. A. Duarte, R. A. Nome, W. R. Rocha and T. A. S. Brandao, *Phys. Chem. Chem. Phys.*, 2015, **17**, 2404-2415.
- 25 C. C. Bott and T. Kurucsev, *J. Chem. Soc., Faraday Trans. 2*, 1975, **71**, 749-755.
- 26 I. B. Beriman, *Handbook of Florescence Spectra of Aromatic Molecules*, 2nd ed., Academic Press, N. Y., 1971.
- 27 a) L. P. Hammett, *J. Am. Chem. Soc.*, 1937, **59**, 96-103; b) C. Hansch, A. Leo and R. W. Taft, *Chem. Rev.*, 1991, **91**, 165-195.
- 28 H. Takai, A. Odani and Y. Sasaki, *Chem. Pharm. Bull.*, 1978, **26**, 1672-1676.
- 29 E. A. Steck, G. W. Ewing and F. Nachod, *J. Am. Chem. Soc.*, 1948, **70**, 3397-3406.
- 30 E. W. Driscoll, J. R. Hunt and J. M. Dawlaty, *J. Phys. Chem. Lett.*, 2016, **7**, 2093-2099.
- 31 E. S. Sales, J. M. F. M. Schneider, M. J. L. Santos, A. J. Bortoluzzi, D. R. Cardoso, W. G. Santos and A. A. Merlo, *J. Braz. Chem. Soc.*, 2015, **26**, 562-571.
- 32 M. Kasha, *Discuss. Faraday Soc.*, 1950, **9**, 14-19.
- 33 a) R. Andruzzi, A. Trazza, L. Greci and L. Marchetti, *J. Electroanal. Chem. Interfacial Electrochem.*, 1980, **108**, 49-58; b) K. Alwair and J. Grimshaw, *J. Chem. Soc., Perkin Trans. 2*, 1973, 1811-1815; c) R. E. Cover and J. T. Folliard, *J. Electroanal. Chem. Interfacial Electrochem.*, 1971, **30**, 143-159.
- 34 D. M. W. v. d. Ham, G. F. S. Harrison, A. Spaans and D. V. d. Meer, *Recl. Trav. Chim. Pays-Bas*, 1975, **94**, 168-173.
- 35 K. Izutsu, *Electrochemistry in Nonaqueous Solutions*, Wiley, 2002.
- 36 M. J. Frisch, G. W. Trucks, H. B. Schlegel, G. E. Scuseria, M. A. Robb, J. R. Cheeseman, G. Scalmani, V. Barone, G. A. Petersson, H. Nakatsuji, X. Li, M. Caricato, A. V. Marenich, J. Bloino, B. G. Janesko, R. Gomperts, B. Mennucci, H. P. Hratchian, J. V. Ortiz, A. F. Izmaylov, J. L. Sonnenberg, Williams, F. Ding, F. Lipparini, F. Egidi, J. Goings, B. Peng, A. Petrone, T. Henderson, D. Ranasinghe, V. G. Zakrzewski, J. Gao, N. Rega, G. Zheng, W. Liang, M. Hada, M. Ehara, K. Toyota, R. Fukuda, J. Hasegawa, M. Ishida, T. Nakajima, Y. Honda, O. Kitao, H. Nakai, T. Vreven, K. Throssell, J. A. Montgomery Jr., J. E. Peralta, F. Ogliaro, M. J. Bearpark, J. J. Heyd, E. N. Brothers, K. N. Kudin, V. N. Staroverov, T. A. Keith, R. Kobayashi, J. Normand, K. Raghavachari, A. P. Rendell, J. C. Burant, S. S. Iyengar, J. Tomasi, M. Cossi, J. M. Millam, M. Klene, C. Adamo, R. Cammi, J. W. Ochterski, R. L. Martin, K. Morokuma, O. Farkas, J. B. Foresman and D. J. Fox, Wallingford, CT, 2016.
- 37 M. Caricato, B. Mennucci, J. Tomasi, F. Ingrosso, R. Cammi, S. Corni and G. Scalmani, *J. Chem. Phys.*, 2006, **124**, 124520.
- 38 T. Le Bahers, C. Adamo and I. Ciofini, *J. Chem. Theory Comput.*, 2011, **7**, 2498-2506.

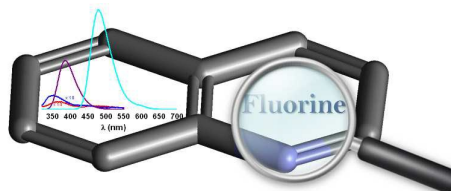


New Journal of Chemistry

Graphical Abstract

A Physico-chemical Investigation on Fluorine-Enriched Quinolines

F. Aribi, A. Panossian, D. Jacquemin, J.-P. Vors, S. Pazenok, F. Leroux, M. Elhabiri



A homogenous series of 2,4-bis(fluoroalkyl)-substituted quinolines was synthesized under mild reaction conditions and their physico-chemical (absorption and emission, electrochemistry, TD-DFT) properties were thoroughly investigated.